blood advances

TO THE EDITOR:

Shared and distinct genetic features in human and canine B-cell lymphomas

Krysta Mila Coyle,[1,*] Tiana Hillman,[1,*] Matthew Cheung,[1] Bruno M. Grande,[1] Kevin R. Bushell,[1] Sarah E. Arthur,[1] Miguel Alcaide,[1] Nicole Thomas,[1] Kostiantyn Dreval,[1] Stephanie Wong,[1] Krishanna Campbell,[1] and Ryan D. Morin[1-3]

[1]Department of Molecular Biology and Biochemistry, Simon Fraser University, Burnaby, BC, Canada; and [2]Genome Sciences Centre, and [3]Lymphoid Cancer Research, BC Cancer, Vancouver, BC, Canada

Animal models of human cancers are an important tool for the development and preclinical evaluation of therapeutics. Canine B-cell lymphoma (cBCL) is an appealing alternative to murine preclinical models because of its frequent, spontaneous incidence and its clinical and histological similarities to some human mature B-cell neoplasms.[1,2] Dogs are particularly relevant for comparative oncology, as they show a higher sequence similarity in cancer genes to humans, relative to mice, and telomerase is largely inactive in adult dog tissues, as in humans.[3,4] Current veterinary care for cBCL includes many of the same chemotherapeutic agents used for human B-cell lymphomas (hBCLs), and the accelerated lifespan of dogs and relative acceleration in cancer progression may allow for more rapid observations of experimental treatments.[1,5,6] Of note, trials of the Bruton tyrosine kinase inhibitors ibrutinib[6] and acalabrutinib[7] in canines provided evidence of clinical efficacy before the first in-human studies. Subsequent approval of these inhibitors for treatment of hBCLs speaks to the relevance of canine models.

The most common form of cBCL resembles human diffuse large B-cell lymphoma (hDLBCL),[3] with other subtypes, including Burkitt-like cBCL, less frequently diagnosed.[8,9] Genomic characterization of hDLBCL continues to reveal novel subtypes with different clinical features and responses to therapy.[10] Given the mutation patterns that underlie molecular heterogeneity in hDLBCL, we hypothesized that the molecular heterogeneity of cBCL and its relationship to hDLBCL remains incomplete and is not adequately captured by current diagnostic methods.[11] Moreover, the utility of cBCL as a veterinary model of human disease would be bolstered by an enhanced understanding of the genetic alterations that collectively underlie cBCL.

We obtained fresh frozen and matched plasma/serum from 86 dogs from the Canine Comparative Oncology Genomic Consortium (CCOGC), with 61 confirmed as having BCL by immunophenotyping (supplemental Table 1). Immunophenotype was not available for the remaining samples. We extracted total RNA and DNA from 29 tumor samples and performed RNA sequencing as previously described (supplemental Table 2).[12] Genomic DNA was extracted from the remaining tumors by using either the AllPrep DNA/RNA Universal Kit or the DNeasy Blood and Tissue Kit (Qiagen). DNA was extracted from plasma or serum with the MagMAX Cell-free DNA Isolation Kit (Thermo Fisher, Waltham, MA).

We used STAR to align RNA-seq reads to the canFam3 reference[13] and identified single nucleotide variants and indels, as described previously.[12] After identifying genes with evidence for recurrent mutations, we performed targeted sequencing of candidate mutations using custom polymerase chain reaction (PCR) primers. We produced custom capture baits by PCR amplification of each exon of interest using genomic DNA from a healthy dog as a template.[14] Tumor DNA libraries were prepared by using the QIAseq FX DNA Library Kit (Qiagen). Plasma and serum DNA libraries were prepared with the NebNext Ultra II DNA Library Prep Kit (New England BioLabs), followed by enrichment using our baits. Sequencing data are available through the National Center for Biotechnology Information (NCBI) PRJNA797476. We aligned reads to canFam3.1 and visually confirmed mutations using Geneious. Variants were annotated with Variant Effect Predictor and human-dog pairwise alignments were extracted from Ensembl to identify human positions for all canine variants.

Submitted 22 October 2021; accepted 8 March 2022; prepublished online on *Blood Advances* First Edition 31 March 2022; final version published online 7 June 2022. DOI 10.1182/bloodadvances.2021006429.

*K.M.C. and T.H. contributed equally to this study.

Other data are available by email request to the corresponding author (rdmorin@sfu.ca).

The full-text version of this article contains a data supplement.

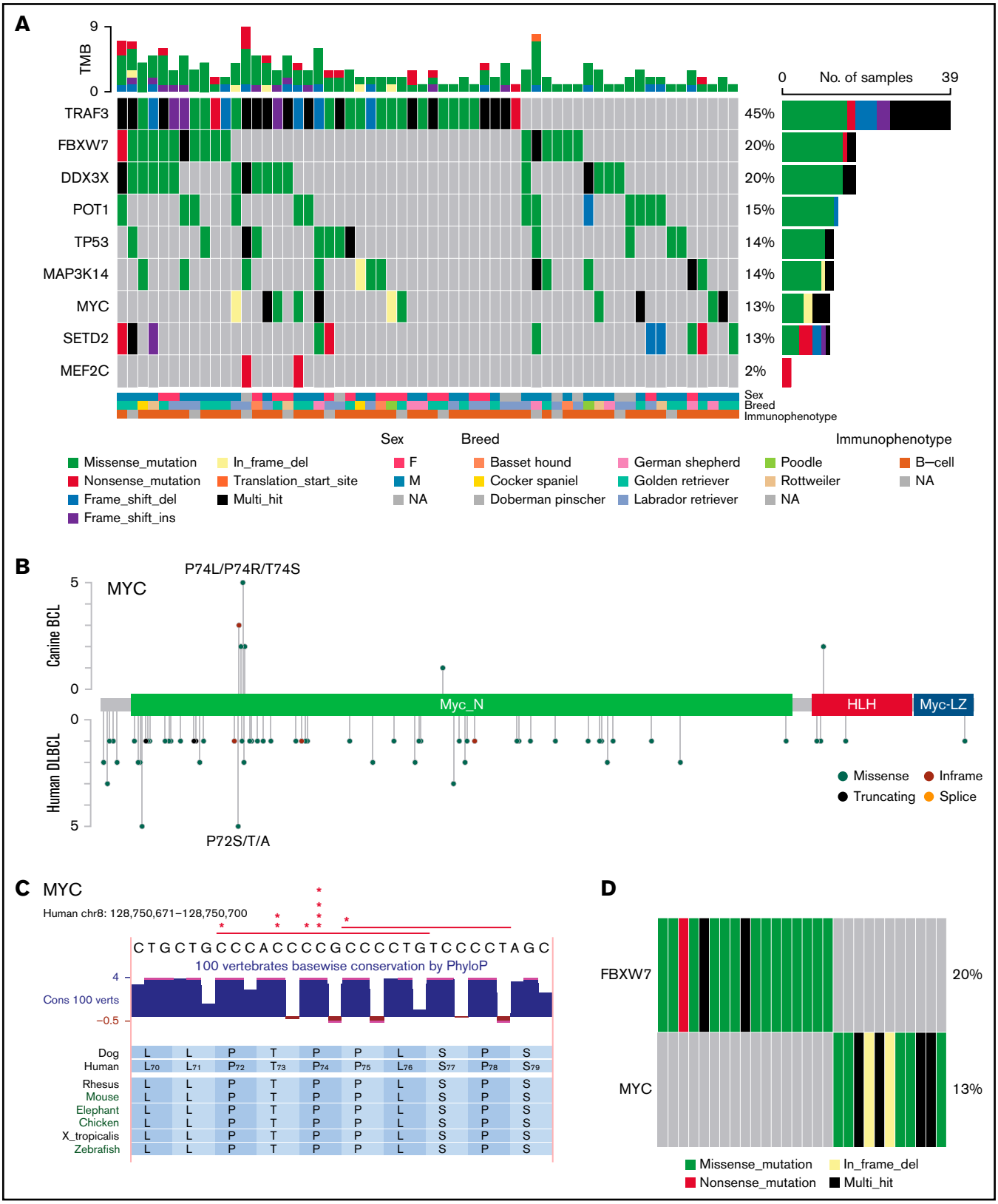
A
TMB
9
0
0
No. of samples
39
TRAF3
FBXW7
DDX3X
POT1
TP53
MAP3K14
MYC
SETD2
MEF2C
45%
20%
20%
15%
14%
14%
13%
13%
2%
Sex
Breed
Immunophenotype
Sex
Breed
Immunophenotype
Missense_mutation
Nonsense_mutation
Frame_shift_del
Frame_shift_ins
In_frame_del
Translation_start_site
Multi_hit
F
M
NA
Basset hound
Cocker spaniel
Doberman pinscher
German shepherd
Golden retriever
Labrador retriever
Poodle
Rottweiler
NA
B–cell
NA
B
MYC
P74L/P74R/T74S
P72S/T/A
Canine BCL
Human DLBCL
5
0
0
5
Myc_N
HLH
Myc-LZ
Missense
Inframe
Truncating
Splice
C
MYC
Human chr8: 128,750,671–128,750,700
C T G C T G C C C A C C C C G C C C C T G T C C C C T A G C
100 vertebrates basewise conservation by PhyloP
4
Cons 100 verts
−0.5
Dog
Human
Rhesus
Mouse
Elephant
Chicken
X_tropicalis
Zebrafish
D
FBXW7
MYC
20%
13%
Missense_mutation
Nonsense_mutation
In_frame_del
Multi_hit

Figure 1.

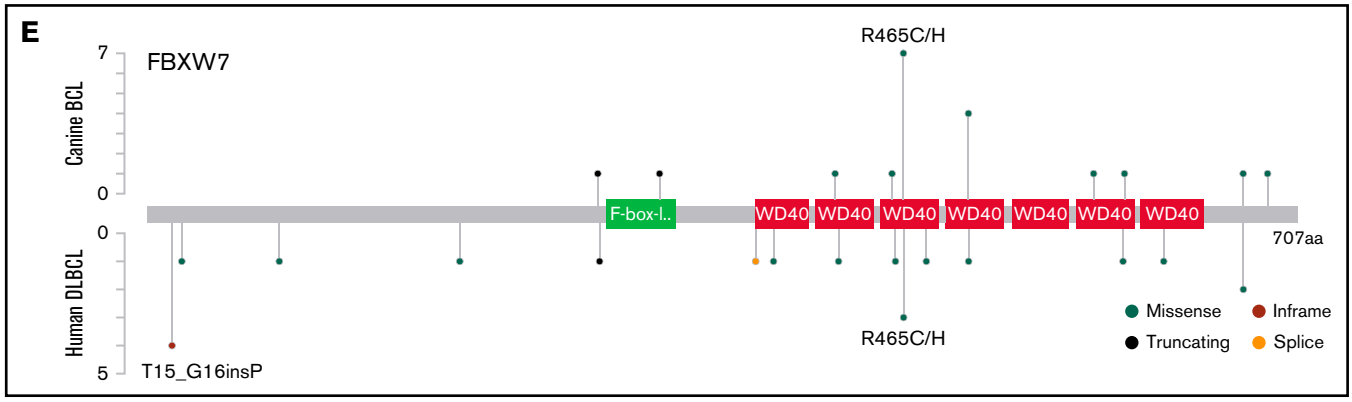

Figure 1 (continued) Targeted sequencing of cBCLs identifies frequent mutations that affect MYC stability. (A) Frequently mutated genes identified in cBCL. Mutations observed across 86 canine BCL samples in 9 genes. After removing suspected germline variants,[12] cBCLs had between 0 and 9 mutations (mean, 2.02) in genes of interest. Mutation frequencies of *POT1* (15%), *TP53* (14%), and *SETD2* (13%) are similar to those reported in previous studies.[15,16] *MAP3K14* mutations occur in 14% of cases; however, its frequency in other studies has not been reported.[15] (B) Spatial distribution of mutations observed in *MYC*, compared with human DLBCL. The odds ratio corresponding to the proportion of *MYC* hotspot mutations in cBCL vs hDLBCL is 30.79 (95% confidence interval [CI], 6.73-202.3; $P = 1.21 \times 10^{-7}$). (C) The *MYC* phosphodegron sequence is highly conserved in vertebrates and the most common site of *MYC* mutations in cBCL (12 of 15 mutations). (D) *MYC* and *FBXW7* mutations do not co-occur in cBCL. (E) Spatial distribution of mutations observed in *FBXW7*, as compared with human DLBCL. The hotspot (present in both human and canine BCL) occurs in a WD40 repeat, which forms one of the blades of the β-propellor and affects a residue forming part of the substrate recognition domain.

Using mutations identified in either tumor or circulating tumor DNA (supplemental Figure 1), we confirmed 9 recurrently mutated genes in cBCL (Figure 1A), including the previously noted high frequency of mutations in *TRAF3* (45%) and *FBXW7* (20%; Figure 1A).[12,15,16] *DDX3X* (20%) and *MYC* (13%) were mutated at a higher frequency than has been previously described in cBCL.[15] These higher rates can be attributed, in part, to our prior observation of high levels of tumor DNA contaminating some of the normal samples.[12]

We compared the pattern and incidence of mutations between cBCL, hDLBCL, and human Burkitt lymphoma (hBL, from a variety of in-house and published sources (supplemental Figure 2).[17-19] *MYC* is commonly deregulated by translocation in hDLBCL and hBL, and these events are commonly associated with point mutations related to aberrant somatic hypermutation.[20] We observed a low frequency of *MYC* mutations in our cBCL cohort with a more focal pattern that is not consistent with the pattern in hDLBCL (Figure 1B). Twelve mutations (80%) affect MYC box I, located in a conserved Cdc4 phosphodegron (CPD) sequence (Figure 1C). In human MYC, these are known to stabilize the protein by rendering it resistant to FBXW7-mediated degradation.[21,22]

FBXW7 mutations are of particular interest, as we never observe both *MYC* and *FBXW7* mutations in cBCL (Figure 1D). The most recurrent *FBXW7* mutation affected R470, corresponding to the human R465 codon, which is also a hot spot in hDLBCL (Figure 1E). These mutations are predicted to yield a dominant negative form of FBXW7 that does not effectively degrade target substrates including MYC and NOTCH1.[23] We hypothesize that mutations in *FBXW7* and the *MYC* CPD represent alternative approaches to stabilizing MYC protein, possibly resulting in overexpression.

DDX3X was one of the most frequently mutated genes in our cohort (20%) and is among the most frequently mutated genes in hBL (46%), but with a strikingly different pattern (supplemental Figure 2). Interestingly, only missense mutations were observed in cBCL, whereas hBLs included a high proportion of truncating mutations (Figure 2A).[24] We explored various clinical features of patients with hBL to identify possible explanations for this difference. Separating *DDX3X* mutations from male and female cases of hBL resolved a similar pattern only in female cases of hBL (Figure 2B), whereas stratification on Epstein-Barr viral status showed no clear pattern (supplemental Figure 3). In males, mutations were found across the entire length of the *DDX3X* coding region with a large proportion of truncating mutations, including both nonsense and frameshift, whereas the pattern in females was predominantly missense mutations affecting the DEAD box and helicase domains. In contrast, although all *DDX3X* mutations in cBCL were missense, there was no sex bias observed in frequency or location (Figure 2C).

DDX3Y, a paralog of *DDX3X*, is encoded on the Y chromosome. Based on high sequence similarity (Figure 2D) and functional evidence, DDX3X and DDX3Y proteins may have partially redundant functions in humans.[24,25] We considered the possibility that DDX3Y plays a compensatory role in males with *DDX3X* mutations. We found a significantly higher expression of DDX3Y in males with hBLs with *DDX3X* mutations when compared with males without these mutations (Figure 2E). A similar comparison was not possible for cBCL because of the small sample size; however, our findings support the premise that these 2 proteins may have functional redundancy in the context of human lymphomagenesis, but may not in canine lymphomagenesis. This represents an important difference between cBCLs and hBCLs.

cBCL has value as an intermediate between rodent models and clinical trials; however, our data identified 2 key factors, *FBXW7* and *DDX3X*, that may promote the use of cBCL as a preclinical model for mature hBCLs. In human cancers, *FBXW7* is most commonly mutated in cholangiocarcinoma and T-cell acute lymphoblastic leukemia,[23] but is rarely observed in the mature B-cell malignancies used in this study. We hypothesize that *FBXW7* mutations in cBCL have a redundant function to the mutations affecting the *MYC* phosphodegron, which may be the cause of the apparent mutual exclusivity observed in this study. This redundancy should be considered in future

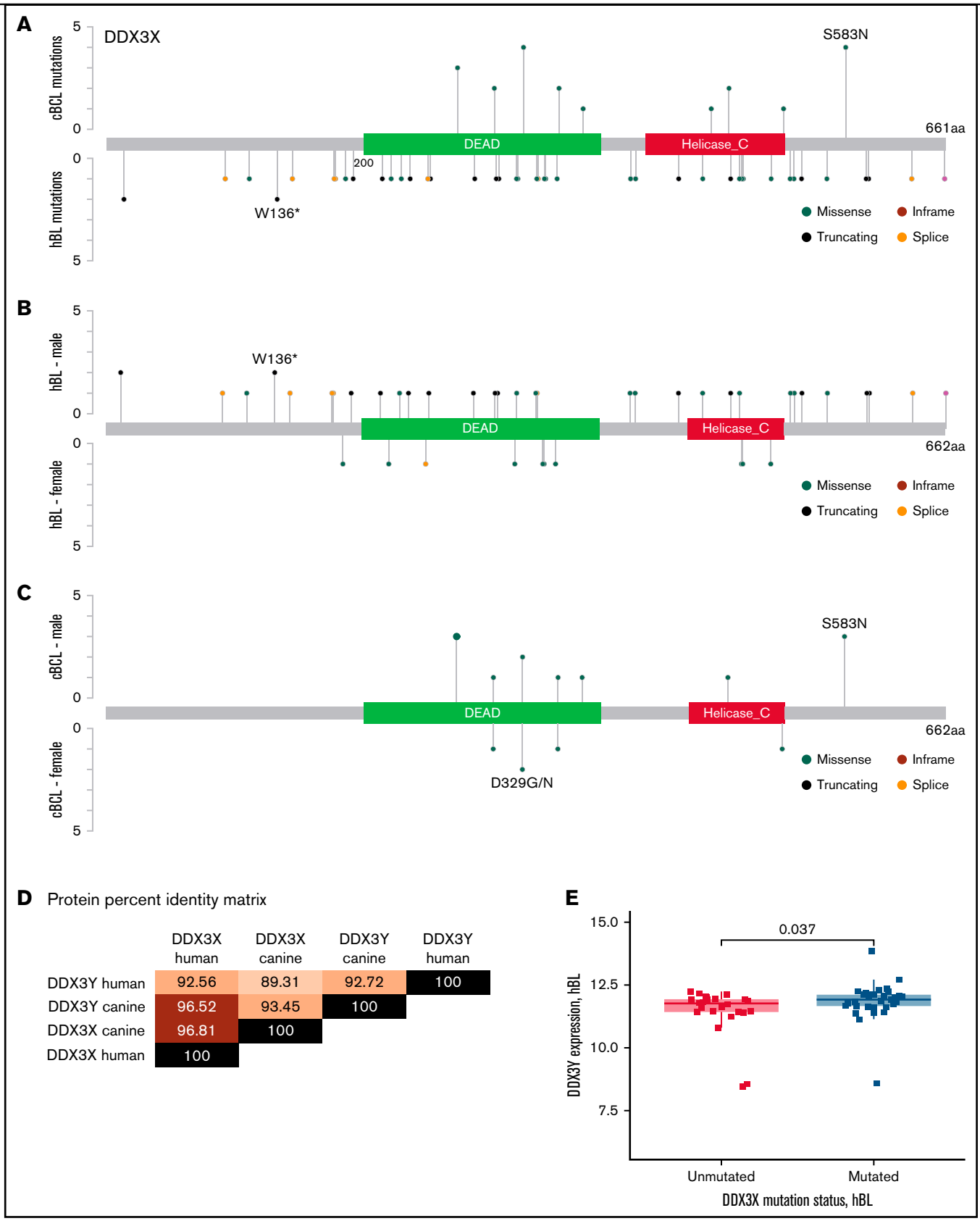
A
DDX3X
cBCL mutations
hBL mutations
5
0
0
5
S583N
661aa
DEAD
Helicase_C
200
W136*
Missense
Inframe
Truncating
Splice
B
hBL - male
hBL - female
W136*
662aa
C
cBCL - male
cBCL - female
S583N
D329G/N
D
Protein percent identity matrix
DDX3X human
DDX3X canine
DDX3Y canine
DDX3Y human
DDX3Y human 92.56 89.31 92.72 100
DDX3Y canine 96.52 93.45 100
DDX3X canine 96.81 100
DDX3X human 100
E
0.037
DDX3Y expression, hBL
15.0
12.5
10.0
7.5
Unmutated
Mutated
DDX3X mutation status, hBL

Figure 2.

studies of potential MYC-targeted therapies for canine lymphomas. Although differences in hBL *DDX3X* mutation frequency have been observed between sexes,[24] we are the first to describe a sex-specific pattern of mutations affecting *DDX3X* in hBL; this pattern is not recapitulated in cBCL. The discrepancy in mutation patterns between canines and human represents an important distinction that may indicate differences in the biology of these cancers

This study revealed key differences in the mutational profiles of cBCLs and hBCLs and provides an impetus for enhanced genomic characterization of canine lymphomas, particularly in their continued use as a preclinical model for human disease. The relevance of canine models will vary, depending on the intervention being pursued, and these findings may diminish the utility of canine models for future clinical studies of targeted agents in DLBCL.

Acknowledgments: The authors thank the Canine Comparative Oncology Genomics Consortium (CCOCG; Broad Institute, Boston MA) for providing the canine tissue samples and Jovanveer Shoker for technical contributions.

This work was supported by a Natural Sciences and Engineering Research Council (NSERC) discovery grant and a Genome Canada contract, and start-up funds were provided by the BC Cancer Foundation (R.D.M.). R.D.M. is a Michael Smith Scholar. K.M.C. is supported by a Canadian Institute of Health research (CIHR) Postdoctoral Fellowship.

The Genomic Variation in Diffuse Large B Cell Lymphomas study was supported by the Intramural Research Program of the National Cancer Institute, National Institutes of Health, Department of Health and Human Services. The datasets have been accessed through the NIH database for Genotypes and Phenotypes (dbGaP, accession number phs001444). A full list of acknowledgements can be found in the supplementary note (Schmitz et al).[17] This work is conducted as part of the Slim Initiative for Genomic Medicine (SIGMA), a joint U.S.-Mexico project funded by the Carlos Slim Health Institute. Data is available at dbGAP (accession number phs000450). The results published here are in whole or part based upon data generated by the Cancer Genome Characterization Initiative (phs000235, Non-Hodgkin Lymphoma project), developed by the NCI. The data used for this analysis are available at https://www.ncbi.nlm.nih.gov/projects/gap/cgi-bin/study.cgi?study_id=phs000235.v6.p1. Information about CGCI projects can be found at https://ocg.cancer.gov/programs/cgci.

Contribution: K.M.C. and R.D.M. prepared the manuscript; K.M.C., K.R.B., B.M.G., and R.D.M. conceived and designed experiments; T.H., K.R.B., M.C., S.E.A., N.T., K.D., M.A., S.W., and K.C. performed the experiments; and K.C., T.H., M.C., B.M.G., K.R.B., N.T., K.D., and R.D.M. performed the analysis and visualization of the data.

Conflict-of-interest disclosure: R.D.M. is a coinventor on patents using genetics and gene expression features to classify lymphomas and is a consultant for Celgene. K.M.C. is a consultant for LM BioStat Consulting Inc. The remaining authors declare no competing financial interests.

ORCID profiles: K.M.C., 0000-0002-1309-4873; B.M.G., 0000-0002-4621-1589; S.E.A., 0000-0002-5341-7868; R.D.M., 0000-0003-2932-7800.

Correspondence: Ryan D. Morin, Simon Fraser University, 8888 University Dr, Burnaby, BC V5A 1S6, Canada; e-mail: rdmorin@sfu.ca; and Krysta M. Coyle, Simon Fraser University, 8888 University Dr, Burnaby, BC V5A 1S6, Canada; e-mail: kcoyle@sfu.ca.

References

1. Hansen K, Khanna C. Spontaneous and genetically engineered animal models: use in preclinical cancer drug development. *Eur J Cancer.* 2004;40(6):858-880.
2. Modiano JF, Breen M, Burnett RC, et al. Distinct B-cell and T-cell lymphoproliferative disease prevalence among dog breeds indicates heritable risk. *Cancer Res.* 2005;65(13):5654-5661.
3. Rowell JL, McCarthy DO, Alvarez CE. Dog models of naturally occurring cancer. *Trends Mol Med.* 2011;17(7):380-388.
4. Nasir L, Devlin P, Mckevitt T, Rutteman G, Argyle DJ. Telomere lengths and telomerase activity in dog tissues: a potential model system to study human telomere and telomerase biology. *Neoplasia.* 2001;3(4):351-359.
5. Kimmelman J, Nalbantoglu J. Faithful companions: a proposal for neurooncology trials in pet dogs. *Cancer Res.* 2007;67(10):4541-4544.
6. Honigberg LA, Smith AM, Sirisawad M, et al. The Bruton tyrosine kinase inhibitor PCI-32765 blocks B-cell activation and is efficacious in models of autoimmune disease and B-cell malignancy. *Proc Natl Acad Sci USA.* 2010;107(29):13075-13080.
7. Harrington BK, Gardner HL, Izumi R, et al. Preclinical evaluation of the novel BTK inhibitor acalabrutinib in canine models of B-cell non-Hodgkin lymphoma. *PLoS One.* 2016;11(7):e0159607.
8. Zandvliet M. Canine lymphoma: a review. *Vet Q.* 2016;36(2):76-104.
9. Aresu L, Agnoli C, Nicoletti A, et al. Phenotypical characterization and clinical outcome of canine Burkitt-like lymphoma. *Front Vet Sci.* 2021;8:647009.
10. Morin RD, Arthur SE, Hodson DJ. Molecular profiling in diffuse large B-cell lymphoma: why so many types of subtypes? *Br J Haematol.* 2022;196(4):814-829.
11. Valli VE, San Myint M, Barthel A, et al. Classification of canine malignant lymphomas according to the World Health Organization criteria. *Vet Pathol.* 2011;48(1):198-211.
12. Bushell KR, Kim Y, Chan FC, et al. Genetic inactivation of TRAF3 in canine and human B-cell lymphoma. *Blood.* 2015;125(6):999-1005.
13. Dobin A, Davis CA, Schlesinger F, et al. STAR: ultrafast universal RNA-seq aligner. *Bioinformatics.* 2013;29(1):15-21.
14. Alcaide M, Rushton C, Morin RD. Ultrasensitive detection of circulating tumor DNA in lymphoma via targeted hybridization

Figure 2 (continued) Sex-specific pattern of DDX3X mutations in hBL is not replicated in cBCL. (A) Spatial distribution of mutations observed in *DDX3X*, compared with hBL. (B) Spatial distribution of *DDX3X* mutations in male and female cases of hBL. The odds ratio corresponding to the presence of truncating mutations in male cases of BL is infinite (95% confidence interval [CI], 1.44-Inf; $P = .00918$). (C) Spatial distribution of DDX3X mutations in canine male and female cBCLs. (D) Protein percentage identity, calculated by Clustal Ω, is highly similar between human and canine *DDX3X* and the Y-linked paralog *DDX3Y*. (E) Expression of *DDX3Y* mRNA is significantly higher in male hBL when a mutation in *DDX3X* is present.

capture and deep sequencing of barcoded libraries. *Methods Mol Biol.* 2019;1956:383-435.

15. Elvers I, Turner-Maier J, Swofford R, et al. Exome sequencing of lymphomas from three dog breeds reveals somatic mutation patterns reflecting genetic background. *Genome Res.* 2015;25(11):1634-1645.
16. Smith PAD, Waugh EM, Crichton C, Jarrett RF, Morris JS. The prevalence and characterisation of TRAF3 and POT1 mutations in canine B-cell lymphoma. *Vet J.* 2020;266:105575.
17. Schmitz R, Wright GW, Huang DW, et al. Genetics and pathogenesis of diffuse large B-cell lymphoma. *N Engl J Med.* 2018;378(15):1396-1407.
18. Chapuy B, Stewart C, Dunford AJ, et al. Molecular subtypes of diffuse large B cell lymphoma are associated with distinct pathogenic mechanisms and outcomes [published correction appears in *Nat Med*. 2018;24(8):1292]. *Nat Med.* 2018;24(5):679-690.
19. Grande BM, Gerhard DS, Jiang A, et al. Genome-wide discovery of somatic coding and noncoding mutations in pediatric endemic and sporadic Burkitt lymphoma. *Blood.* 2019;133(12):1313-1324.
20. Khodabakhshi AH, Morin RD, Fejes AP, et al. Recurrent targets of aberrant somatic hypermutation in lymphoma. *Oncotarget.* 2012;3(11):1308-1319.
21. Welcker M, Orian A, Jin J, et al. The Fbw7 tumor suppressor regulates glycogen synthase kinase 3 phosphorylation-dependent c-Myc protein degradation [published correction appears in *Proc Natl Acad Sci USA*. 2006;103(2):504]. *Proc Natl Acad Sci USA.* 2004;101(24):9085-9090.
22. Yada M, Hatakeyama S, Kamura T, et al. Phosphorylation-dependent degradation of c-Myc is mediated by the F-box protein Fbw7. *EMBO J.* 2004;23(10):2116-2125.
23. Akhoondi S, Sun D, von der Lehr N, et al. FBXW7/hCDC4 is a general tumor suppressor in human cancer [published correction appears in]. *Cancer Res.* 2007;67(19):9006-9012.
24. Gong C, Krupka JA, Gao J, et al. Sequential inverse dysregulation of the RNA helicases DDX3X and DDX3Y facilitates MYC-driven lymphomagenesis. *Mol Cell.* 2021;81(19):4059-4075.e11.
25. Venkataramanan S, Gadek M, Calviello L, Wilkins K, Floor S. DDX3X and DDX3Y are redundant in protein synthesis. *RNA.* 2021;27(12):1577-1588.